consisting of 160 transients recorded over 2048 data points. Four dummy scans were included before each experiment, and a nonspinning sample was used to minimize artifacts in the spectrum. The data was multiplied by Lorentzian line-broadening functions and zero filled to 1024 data points in f_1 prior to transformation.

Acknowledgment. We thank SERC for financial support. This research was carried out within the Cambridge Centre for Molecular Recognition.

Registry No. UK-69542, 133071-47-3.

Siroheme Model Compounds: Vibrational Spectra and Normal Modes of Copper(II) Octaethylisobacteriochlorin

Alexander D. Procyk and David F. Bocian*

Contribution from the Department of Chemistry, Carnegie Mellon University, Pittsburgh, Pennsylvania 15213. *Received November 14, 1990*

Abstract: Resonance Raman (RR) and infrared spectra are reported for the Cu(II) complexes of octaethylisobacteriochlorin (OEiBC) and the *meso*-deuteriated compounds OEiBC-γ-d_1, OEiBC-β,γ,δ-d_3, and OEiBC-$\alpha,\beta,\gamma,\delta$-$d_4$. These compounds represent a series in which each of the three symmetry inequivalent methine bridges of the macrocycle is systematically perturbed. The RR spectra of the complexes are obtained at a variety of excitation wavelengths which span the B_x, B_y, Q_x, and Q_y absorption bands of the complexes. The observed RR intensity enhancement patterns provide insight into the scattering mechanisms that are active for the tetrahydroporphyrin macrocycle. All of the vibrational data are used in conjunction with semiempirical normal coordinate calculations to obtain a set of assignments for the observed high-frequency (above 1000 cm^{-1}), in-plane skeletal modes of CuOEiBC. The normal coordinate calculations and, more importantly, the isotope-shift patterns observed for the complexes deuteriated at specific methine bridges indicate that the forms of the vibrational eigenvectors of many of the modes of the OEiBC macrocycle differ substantially from those of porphyrins, chlorins, or bacteriochlorins. The differences in the general appearance of the vibrational eigenvectors of these various classes of macrocycles can be rationalized in terms of structural changes that occur upon reduction of the pyrrole rings.

I. Introduction

Metallohydroporphyrins (porphyrins with one or more reduced pyrrole rings) serve as the prosthetic groups in a number of proteins which perform a variety of biological functions. Metallochlorins (one reduced pyrrole ring) are found in the photosynthetic proteins of green plants (chlorophylls),[1] leukocyte myeloperoxidase,[2-8] bacterial heme *d*,[9,10] and sulfmyoglobin and sulfhemoglobin.[6,11-17] Metallobacteriochlorins (two opposite reduced pyrrole rings) constitute the active sites in bacterial photosynthetic systems (bacteriochlorophylls),[18,19] whereas metalloisobacteriochlorins (two adjacent reduced pyrrole rings) are found in assimilatory nitrite reductase of green plants[20-22] as well as in the nitrite and sulfite reductases of bacteria.[23-26] A metallocorphinoid (four reduced pyrrole rings) constitutes the methylreductase cofactor, F_{430}, of methanogenic bacteria.[27-29] Presumably, the unique ring structures found in these various metallohydroporphyrin prosthetic groups impart more efficacious biological activity to the specific systems.

Resonance Raman (RR) spectroscopy has proven to be a useful probe of the structural properties of metallohydroporphyrins both in model compounds and in proteins (for a review, see ref 30). The metallochlorins are the most extensively investigated class of metallohydroporphyrins. Vibrational assignments have been proposed for these complexes[31-38] and their vibrational frequencies

(1) Svec, W. A. In *The Porphyrins*; Dolphin, D., Ed.; Academic Press: New York, 1978; Vol. 5, pp 341-349.
(2) Babcock, G. T.; Ingle, R. T.; Oertling, W. A.; Davis, J. C.; Averill, B. A.; Hulse, C. L.; Stufkens, D. J.; Bolscher, B. G. J. M.; Wever, R. *Biochim. Biophys. Acta* **1985**, *828*, 58-66.
(3) Sibbet, S. S.; Hurst, J. K. *Biochemistry* **1984**, *23*, 3007-3013.
(4) Eglington, D. G.; Barber, D.; Thomson, A. J.; Greenwood, C.; Segal, A. W. *Biochim. Biophys. Acta* **1982**, *703*, 187-195.
(5) Morell, D. B.; Chang, Y.; Henry, I.; Nichol, A. W.; Clezy, P. S. In *Structure and Function of Cytochromes*; Okunuki, K., Kamen, M. D., Sezuku, I., Eds.; University Park Press: Baltimore, 1968; pp 563-571.
(6) Morell, D. B.; Chang, Y.; Clezy, P. S. *Biochim. Biophys. Acta* **1967**, *136*, 121-130.
(7) Newton, N.; Morell, D. B.; Clarke, L. *Biochim. Biophys. Acta* **1965**, *96*, 463-475.
(8) Newton, N.; Morell, D. B.; Clarke, L.; Clezy, P. S. *Biochim. Biophys. Acta* **1965**, *96*, 476-486.
(9) Timkovich, R.; Cork, M. S.; Gennis, R. B.; Johnson, P. Y. *J. Am. Chem. Soc.* **1985**, *107*, 6069-6075.
(10) Lemberg, R.; Barret, J. *Cytochromes*; Academic Press: New York, 1973; pp 233-245.
(11) Chatfield, M. J.; La Mar, G. M.; Smith, K. N.; Leung, H.-K.; Pandy, R. K. *Biochemistry* **1965**, *27*, 1500-1507.
(12) Bondoc, L. L.; Chau, M.-H.; Price, M. A.; Timkovich, R. *Biochemistry* **1986**, *25*, 8458-8466.
(13) Chatfield, M. J.; La Mar, G. N.; Lecomte, J. T. J.; Balch, A. L.; Smith, K. M.; Langry, K. C. *J. Am. Chem. Soc.* **1986**, *108*, 7108-7110.
(14) Andersson, L. A.; Loehr, T. M.; Lim, A. R.; Mauk, A. G. *J. Biol. Chem.* **1984**, *259*, 15340-15349.
(15) Peisach, J.; Blumberg, W. E.; Adler, A. *Ann. N.Y. Acad. Sci.* **1973**, *206*, 310-327.
(16) Berofsky, J. A.; Peisach, J.; Blumberg, W. E. *J. Biol. Chem.* **1971**, *246*, 3367-3377.
(17) Brittain, T.; Greenwood, C.; Barber, D. *Biochim. Biophys. Acta* **1982**, *705*, 26-32.
(18) Okamura, M. Y.; Feher, G.; Nelson, N. In *Photosynthesis*; Godvindjee, Ed.; Academic Press: New York, 1982; Vol. I, pp 195-272.
(19) Feher, G.; Okamura, M. Y. In *The Photosynthetic Bacteria*; Clayton, R. K., Sistron, W. R., Eds.; Plenum Press: New York, 1978; pp 349-386.
(20) Lancester, J. R.; Vega, J. M.; Kamin, H.; Orme-Johnson, N. R.; Orme-Johnson, W. H.; Kreuger, R. H.; Siegel, L. M. *J. Biol. Chem.* **1979**, *254*, 1268-1272.
(21) Vega, J. M.; Kamin, H. *J. Biol. Chem.* **1977**, *252*, 896-909.
(22) Murphy, M. J.; Siegel, L. M.; Tover, S. R.; Kamin, H. *Proc. Natl. Acad. Sci. U.S.A.* **1974**, *71*, 612-616.
(23) Andersson, L. A.; Sotiriou, C.; Chang, C. K.; Loehr, T. M. *J. Am. Chem. Soc.* **1987**, *109*, 258-264.
(24) Scott, A. I.; Irwin, A. J.; Siegel, J. M.; Schoolery, J. N. *J. Am. Chem. Soc.* **1978**, *100*, 316-318, 7987-7994.
(25) Siegel, J. M.; Rueger, D. C.; Barber, M. J.; Krueger, R. J.; Orme-Johnson, N. R.; Orme-Johnson, W. H. *J. Biol. Chem.* **1982**, *257*, 6343-6350.
(26) McRee, D. E.; Richardson, D. C.; Richardson, J. S.; Siegel, L. M. *J. Biol. Chem.* **1986**, *261*, 10277-10281.
(27) Wolfe, R. S. *Trends Biochem. Sci. Pres. Edn.* **1985**, *10*, 369-399.
(28) Ellefson, W. L.; Whitman, W. B.; Wolfe, R. S. *Proc. Natl. Acad. Sci. U.S.A.* **1982**, *79*, 3707-3710.
(29) Pfaltz, A.; Juan, B.; Fassler, A.; Eschenmoser, A.; Jaenchen, R.; Gilles, H. H.; Diekert, G.; Thauer, R. K. *Helv. Chim. Acta* **1982**, *65*, 828-865.
(30) Schick, G. A.; Bocian, D. F. *Biochim. Biophys. Acta* **1987**, *895*, 127-154.
(31) Ozaki, Y.; Kitagawa, T.; Ogoshi, H. *Inorg. Chem.* **1979**, *18*, 1772-1776.
(32) (a) Ozaki, Y.; Iriyama, K.; Ogoshi, H.; Ochiai, T.; Kitagawa, T. *J. Phys. Chem.* **1986**, *90*, 6105-6112. (b) Ozaki, Y.; Iriyama, K.; Ogoshi, H.; Ochiai, T.; Kitagawa, T. *J. Phys. Chem.* **1986**, *90*, 6113-6118.
(33) (a) Fujiwara, M.; Tasumi, M. *J. Phys. Chem.* **1986**, *90*, 250-255. (b) Fujiwara, M.; Tasumi, M. *J. Phys. Chem.* **1986**, *90*, 5646-5650.

0002-7863/91/1513-3765$02.50/0

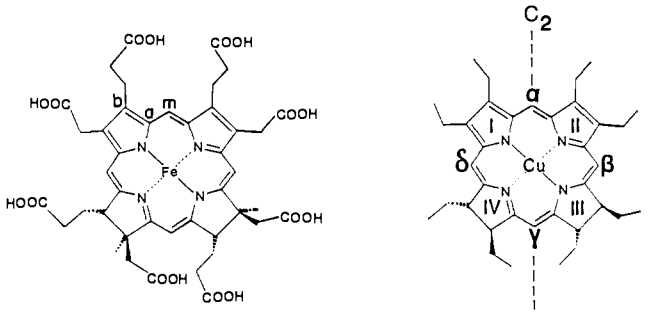

Figure 1. Structure and labeling scheme for siroheme (left) and CuOEiBC (right).

have been examined as a function of the coordinated metal ions and, for iron systems, the oxidation and spin states of the metal.[31-33,39] Normal coordinate calculations have also been performed on metallochlorins.[37,40,41] Calculations by our group predict that the forms of the vibrational eigenvectors of a number of the structure-sensitive, high-frequency skeletal modes of these complexes are substantially different from those of metalloporphyrins.[37,40] [For a different point of view, see ref 41.] Babcock and co-workers have recently performed extensive specific deuteriation studies on MOEC complexes (OEC = octaethylchlorin) that confirm the prediction that the vibrational eigenvectors of porphyrins and chlorins are different.[42] Consequently, the vibrational frequency–structure correlations that have been developed for metalloporphyrins must be applied with caution to metallochlorins.

In contrast with the substantial number of RR investigations on metallochlorins, far fewer vibrational studies have been conducted on metallotetrahydroporphyrins. Most of this work has focused on bacteriochlorophyll or bacteriochlorophyll model compounds.[40,43-45] Only a few RR studies have been conducted on metalloisobacteriochlorins. Cotton and co-workers[46] and Ondrias and co-workers[47] have examined the RR spectra of heme d_1, while Andersson and co-workers[48,49] have investigated various metalloisobacteriochlorin model complexes. Ondrias et al.[50] have also reported RR spectra of the spinach nitrite reductase which contains a siroheme prosthetic group (Figure 1).[22] More recently,

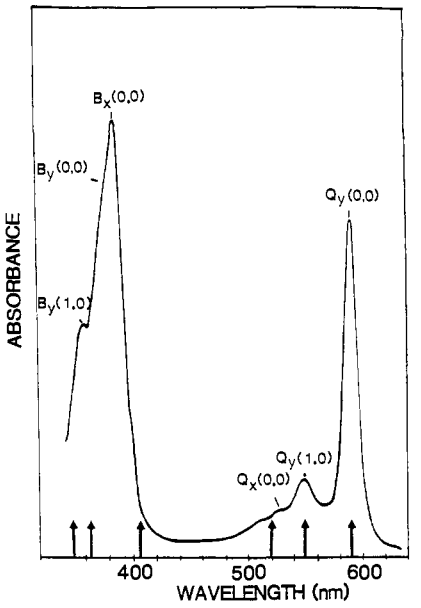

Figure 2. Electronic absorption spectrum of CuOEiBC in benzene. The arrows denote the excitation wavelengths used in the RR studies.

Spiro and co-workers have reported a detailed RR study of a bacterial sulfite reductase which also contains a siroheme moiety.[51] RR spectra have also been reported for the metal-free sirohydrochlorin prosthetic group found in certain other bacterial sulfite reductases.[52] In both of these studies, vibrational assignments were proposed for certain of the high-frequency skeletal modes of the sirohydrochorin macrocycle. However, these assignments were made either by empirical symmetry reduction arguments or by direct analogy to the vibrational assignments of metalloporphyrins. Neither of these approaches provides a detailed picture of the vibrational characteristics of the tetrahydroporphyrin macrocycle. Indeed, a preliminary vibrational study of CuOEiBC (OEiBC = octaethylisobacteriochlorin; Figure 1) by our group suggests that the normal modes of the MOEiBC ring system are different from those of either MOEC or MOEP (OEP = octaethylporphyrin) complexes.[53]

In this paper, we report a detailed vibrational analysis of CuOEiBC. This analysis makes use of several specifically *meso*-deuteriated compounds that were not available at the time of our preliminary RR study of the complex. These include OEiBC-γ-d_1, OEiBC-β,γ,δ-d_3, and OEiBC-$\alpha,\beta,\gamma,\delta$-$d_4$. These compounds represent a series in which each of the three symmetry inequivalent methine bridges of the OEiBC ring is systematically perturbed. In the course the investigations, we obtained RR spectra of CuOEiBC and the three isotopomers by using a variety of excitation wavelengths which span the B_x, B_y, Q_x, and Q_y absorption bands (Figure 2). The IR spectra of the four complexes are also examined. These vibrational data are used in conjunction with semiempirical normal coordinate calculations to obtain a set of assignments for all of the observed high-frequency (above 1000 cm^{-1}), in-plane skeletal modes of CuOEiBC.

II. Methods

A. Experimental Procedures. *trans*-OEiBC and CuOEiBC were synthesized and purified according to the procedure of Stolzenberg et al.[54] Purity was monitored via absorption and nuclear magnetic resonance (NMR) spectroscopy. All of the deuteriated derivatives were prepared by soaking OEiBC in various deuteriated acids for extended periods of time (see below). The products were isolated by pouring the solutions into 25 mL of cold D_2O, extracting with CH_2Cl_2, neutralizing with

(34) Andersson, L. A.; Loehr, T. M.; Cotton, T. M.; Simpson, D. J.; Smith, K. M. *Biochim. Biophys. Acta* **1989**, *974*, 163-179.
(35) (a) Andersson, L. A.; Loehr, T. M.; Chang, C. K.; Mauk, A. G. *J. Am. Chem. Soc.* **1985**, *107*, 182-191. (b) Andersson, L. A.; Loehr, T. M.; Sotiriou, C.; Wu, W.; Chang, C. K. *J. Am. Chem. Soc.* **1986**, *108*, 2908-2916.
(36) Andersson, L. A.; Sotiriou, C.; Chang, C. K.; Loehr, T. M. *J. Am. Chem. Soc.* **1987**, *109*, 258-264.
(37) Boldt, N. J.; Donohoe, R. J.; Birge, R. R.; Bocian, D. F. *J. Am. Chem. Soc.* **1987**, *109*, 2284-2298.
(38) Boldt, N. J.; Bocian, D. F. *J. Phys. Chem.* **1988**, *92*, 581-586.
(39) Ogoshi, H.; Watanabe, E.; Yoshida, Z.; Kincaid, J.; Nakamoto, K. *Inorg. Chem.* **1975**, *14*, 1344-1350.
(40) Donohoe, R. J.; Atamian, M.; Bocian, D. F. *J. Phys. Chem.* **1989**, *93*, 2244-2252.
(41) Prendergast, K.; Spiro, T. G. *J. Phys. Chem.* **1991**, *95*, 1555-1563.
(42) Fonda, H. N.; Oertling, W. A.; Salehi, A.; Chang, C. K.; Babcock, G. T. *J. Am. Chem. Soc.* **1990**, *112*, 9497-9507.
(43) (a) Lutz, M. In *Advances in Infrared and Raman Spectroscopy*; Clark, R. J. H., Hester, R. E., Eds.; Wiley: New York, 1984; Vol. 11, pp 211-300. (b) Lutz, M.; Robert, B. In *Biological Applications of Raman Spectroscopy*; Spiro, T. G., Ed.; Wiley: New York, 1988; Vol. III, pp 347-411.
(44) (a) Cotton, T. M.; Van Duyne, R. P. *J. Am. Chem. Soc.* **1981**, *103*, 6020-6026. (b) Callahan, P. M.; Cotton, T. M. *J. Am. Chem. Soc.* **1987**, *109*, 7001-7007.
(45) Donohoe, R. J.; Frank, H. A.; Bocian, D. F. *Photochem. Photobiol.* **1988**, *48*, 531-537.
(46) Cotton, T. M.; Timkovich, R.; Cork, M. S. *FEBS Lett.* **1981**, *133*, 39-44.
(47) Ching, Y.; Ondrias, M. R.; Rousseau, D. L.; Muhoberac, B. B.; Wharton, D. C. *FEBS Lett.* **1982**, *138*, 239-244.
(48) Andersson, L. A.; Loehr, T. M.; Weishih, W.; Chang, C. K.; Timkovich, R. *FEBS Lett.* **1990**, *267*, 285-288.
(49) Andersson, L. A.; Loehr, T. M.; Thompson, R. G.; Strauss, S. H. *Inorg. Chem.* **1990**, *29*, 2142-2147.
(50) Ondrias, M. R.; Carson, S. D.; Hirasawa, M.; Knaff, D. B. *Biochim. Biophys. Acta* **1985**, *830*, 159-163.
(51) Han, S.; Madden, J. F.; Thompson, R. G.; Strauss, S. H.; Siegel, L. M.; Spiro, T. G. *Biochemistry* **1989**, *28*, 5461-5470.
(52) Lai, K. K.; Yue, K. T. *J. Raman Spectrosc.* **1990**, *21*, 21-26.
(53) Bocian, D. F.; Procyk, A. D.; Peloquin, J. M. *Proc. SPIE* **1989**, *1057*, 146-153.
(54) Stolzenberg, A. M.; Spreer, L. O.; Holm, R. H. *J. Chem. Soc.* **1980**, *102*, 364-371.

$NaHCO_3$ dissolved in D_2O, and washing with D_2O. [The use of H_2O in the isolation procedure was found to result in back-exchange of up to 50% of the incorporated deuterons.] The extent of deuteriation was monitored by proton NMR spectroscopy.

The procedures for obtaining each of the specifically deuteriated compounds were as follows: OEiBC-γ-d_1 was prepared by soaking OEiBC in deoxygenated (via N_2 bubbling) trifluoroacetic acid-*d* for 5 days at −5 °C. These conditions provided the maximum selectivity of γ-exchange as determined by studies in which the type of acid, the temperature, and the soaking time were varied. The extent of deuteriation at the γ-, β,δ-, and α-positions was found to be ~65%, ~30%, and less than 5%, respectively. OEiBC-β,γ,δ-d_3 was prepared by soaking OEiBC in a 50/50 mixture of deoxygenated CH_3OD/DCl for ~48 h at room temperature. The extent of deuteriation at the γ-, β,δ-, and α-positions was determined to be greater than 95%, ~80%, and less than 5%, respectively. OEiBC-$\alpha,\beta,\gamma,\delta$-$d_4$ was prepared by soaking OEiBC in a 50/50 mixture of deoxygenated CH_3OD/D_2SO_4 for ~24 h at room temperature. The extent of deuteriation at the γ-, β,δ-, and α-positions was found to be greater than 95%, ~90%, and ~75%, respectively. Attempts were also made to obtain OEiBC-β,δ-d_2 (via back-exchange of OEiBC-β,γ,δ-d_3 in trifluoroacetic acid) and OEiBC-α-d_1 (via back-exchange of OEiBC-$\alpha,\beta,\gamma,\delta$-$d_4$ in CH_3OH/HCl); however, the extent of selective labeling was not sufficient to be useful in the vibrational studies.

The RR spectra were recorded on a Spex Industries 1403 double monochromator equipped with a thermoelectrically cooled Hammamatsu R928 photomultiplier tube and a photon-counting detection system. Excitation wavelengths were provided by the discrete outputs of an Ar ion (Coherent Radiation Innova 15UV), Kr ion (Coherent Radiation Innova 200-K3), or Ar ion-pumped tunable dye laser (Coherent Radiation 590-03). The dyes used were either Rhodamine 590 or Rhodamine 560 (Exciton Chemical Co.). Unpolarized RR spectra were obtained of samples either dissolved in degassed CH_2Cl_2 (distilled off of P_2O_5) or suspended in compressed pellets (with either Na_2SO_4 or KBr as the supporting medium). Polarized RR spectra were recorded of the samples in solution. Both the solutions (sealed in NMR tubes) and pellets were spun to prevent photodecomposition. [Photooxidation to CuOEC rapidly occurs with blue excitation even with spinning when the solvent is not rigorously purified and oxygen free.] The incident powers were approximately 20 mW with λ_{ex} = 351.1, 363.8, and 406.7 nm and 50 mW with λ_{ex} = 520.8, 550.7, and 591.5 nm. The spectra were collected at 1-cm^{-1} intervals at a rate of 1 s/point. The spectral slit width was ~3 cm^{-1} at all excitation wavelengths.

The IR spectra were recorded on a Nicolet 5DXB FT-IR spectrometer. The samples were dissolved in CCl_4 solutions or suspended in KBr pellets. The path length for the solution studies was 0.014 mm. The spectral resolution was ~2 cm^{-1}.

B. Normal Coordinate Calculations. The vibrational frequencies and normal modes of CuOEiBC were calculated by using the QCFF/PI semiempirical program package.[55] This method determines the ground-state and excited-state potential surfaces based on an empirical σ-potential function and a semiempirical Pariser–Parr–Pople π-electron calculation that includes single excitation configuration interaction. An optimized geometry is produced in the course of orbital energy minimization. In previous studies of chlorophyll and bacteriochlorophyll model compounds, we have found that the QCFF/PI method gives a reasonable description of the geometries, vibrational frequencies, and eigenvectors of these hydroporphyrins.[37,45]

The calculations on CuOEiBC were initiated by inputting a modified version of the crystallographically determined skeletal geometry of 2,2,8,8,12,13,17,18-octamethylisobacteriochlorin.[56] This modification entailed imparting C_2 symmetry (Figure 1) to the crystallographically determined structure (the actual structure deviates somewhat from this geometry). The C_b-ethyl substituents were approximated as 15 amu point masses and were placed in a *ttt*-configuration on the pyrroline rings. The QCFF/PI optimized structure retained C_2 symmetry and exhibited bond lengths which were not appreciably different from those of the input geometry (±0.03 Å). Several other sets of calculations were also performed in order to determine the dependence of the vibrational frequencies and eigenvectors on the exact structure of the macrocycle. For example, the force constants were included such that the average deviation from planarity of the ring skeleton increased by ~0.15 Å. Although this altered the frequencies of the skeletal modes by up to 10 cm^{-1}, the isotopic shifts and forms of the eigenvectors were not substantially affected. Calculations were also performed in which the following modifications were made in the treatment of the ethyl groups: (1) The point masses were varied. (2) The methylene portions of the groups on the pyrrole rings were explicitly included. (3) The substituents were placed in a *ttc*-, *tct*-, *tcc*-, or *ccc*-configuration on the pyrroline rings. This latter study was performed because these R-group configurations (as well as the *ttt* form) are all found on the reduced rings of siroheme (these rings contain three R groups rather than the two present in the OEiBC model complex (Figure 1)). In all cases, the above modifications had only minor effects on the vibrational frequencies and isotopic shifts of the skeletal modes of the macrocycle. The appearance of the vibrational eigenvectors was also unaltered except when the ethyl groups were placed in configurations that do not maintain C_2 symmetry. In these cases, certain of the eigenvectors are skewed with respect to the former C_2 axis. This skewing results from a redistribution of the potential energy distribution among internal coordinates that were formerly equivalent (in C_2 symmetry). However, the loss of symmetry does not result in any new contributions (by other types of internal coordinates) to the normal mode. Accordingly, the isotopic shifts are unaltered despite the change in appearance of the vibrational eigenvectors.

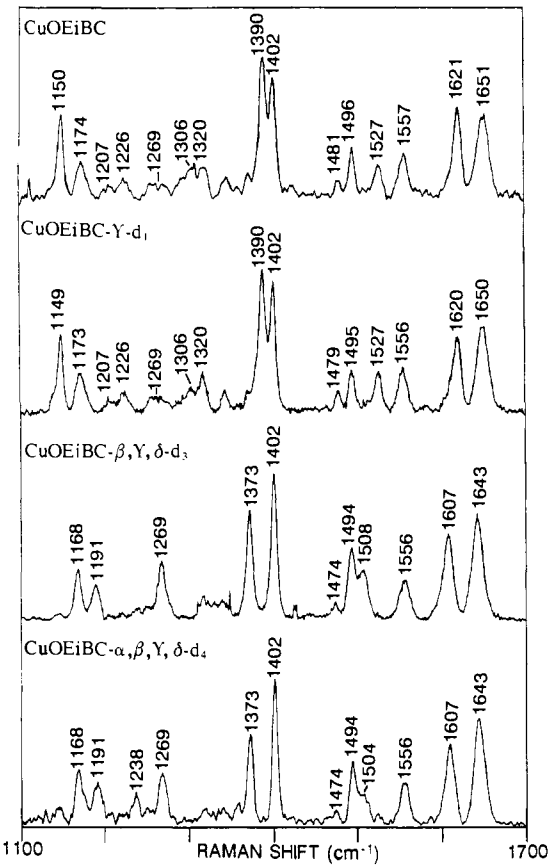

Figure 3. High-frequency regions of the B-state (λ_{ex} = 406.7 nm) RR spectra of CuOEiBC and the three *meso*-deuteriated isotopomers. The spectra are of samples in CH_2Cl_2 solution.

III. Results

A. RR Spectra. Representative high-frequency RR spectra of CuOEiBC and the three isotopomers obtained with $B_x(0,0)$ and $Q_y(1,0)$ excitation are shown in Figures 3 and 4, respectively. The low-frequency RR spectra of the four complexes obtained with $B_x(0,0)$ excitation are shown in Figure 5. The exact excitation wavelengths are given in the figure legends. With $Q_y(1,0)$ excitation, there is little appreciable enhancement of low-frequency modes (not shown). The only exceptions are bands at 734 and 1010 cm^{-1} which are also observed with $B_x(0,0)$ excitation (Figure 5). The RR spectra shown in Figures 3–5 were obtained of samples in CH_2Cl_2 solution. Comparison of these spectra with those obtained of samples in compressed pellets (KBr or Na_2SO_4) reveals that several of the RR frequencies are substantially different in the two media. For example, the bands observed at 1651 and 1621 cm^{-1} in solution downshift to 1643 and 1613 cm^{-1}, respectively, in KBr pellets. Babcock and co-workers have observed similar solid-state effects in their studies of MOEC com-

(55) (a) Warshel, A.; Karplus, M. *J. Am. Chem. Soc.* **1972**, *94*, 5612–5625. (b) Warshel, A.; Levitt, M. *Quantum Chemistry Program Exchange* **1974**, No. 247, Indiana University.

(56) Cruse, W. B. T.; Harrison, P. J.; Kennard, O. *J. Am. Chem. Soc.* **1982**, *104*, 2376.

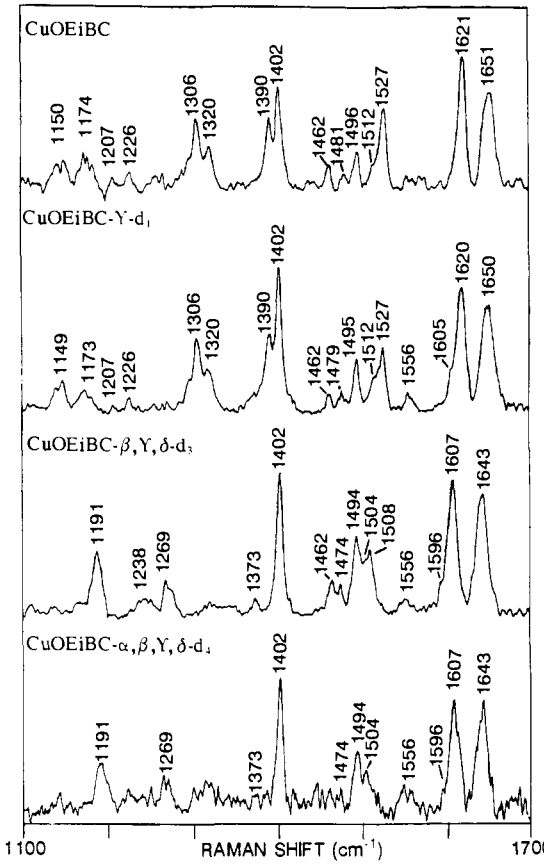

Figure 4. High-frequency regions of the Q-state (λ_{ex} = 550.7 nm) RR spectra of CuOEiBC and the three *meso*-deuteriated isotopomers. The spectra are of samples in CH_2Cl_2 solution.

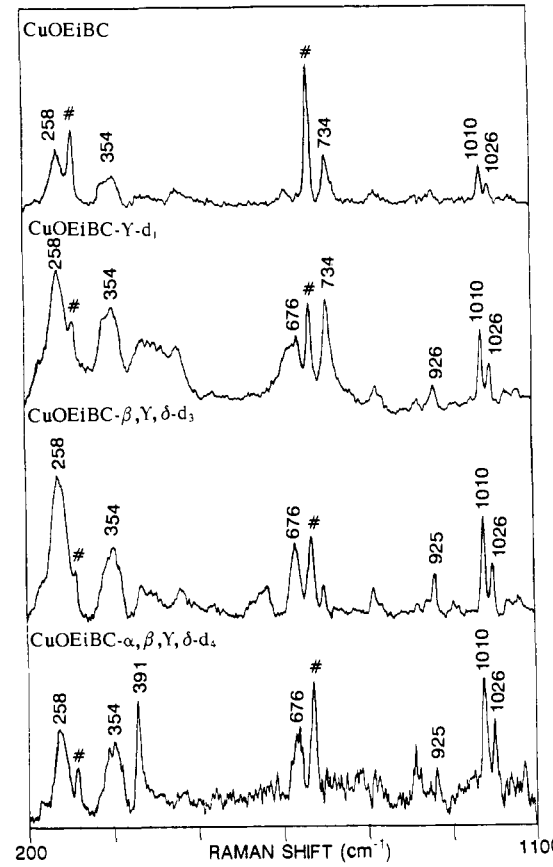

Figure 5. Low-frequency regions of the B-state (λ_{ex} = 406.7 nm) RR spectra of CuOEiBC and the three *meso*-deuteriated isotopomers. The spectra are of samples in CH_2Cl_2 solution. Solvent peaks are indicated by the symbol #.

plexes (unpublished results). These solid-state effects are sufficiently large that it is potentially misleading to compare vibrational spectra recorded in solution versus solid phase. Consequently, we will focus only on the RR (and IR) data acquired in solution.

Comparison of Figures 3 and 4 reveals that the RR intensity enhancement patterns are generally similar with excitation at the two different wavelengths. To explore further the excitation-wavelength sensitivity of the RR enhancement and to facilitate the assignment of the vibrational modes, spectra were also obtained with excitation at a variety of other wavelengths in the B- and Q-state regions (not shown). The various wavelengths used in the RR experiments are denoted by the arrows in Figure 2. With excitation on the blue side of the B-state absorption band, which should be more resonant with the B_y and the B_x transition, the RR enhancement pattern is similar to that shown in Figure 3. In addition, the RR spectra observed with other excitation wavelengths in the Q-state region are similar to those shown in Figure 4. This latter observation suggests that RR scattering with excitation in the region of the weak Q_x absorption is probably dominated by scattering from the strong, nearby Q_y band. It should be noted that our previously reported RR spectra of CuOEiBC exhibited a number of differences with B- versus Q-state excitation.[53] We have subsequently determined that these differences are primarily due to scattering from a CuOEC photooxidation product formed predominantly with UV/violet excitation wavelengths.

The RR spectra obtained for CuOEiBC at the various excitation wavelengths in the B- and Q-state regions all exhibit predominantly polarized (p) and anomalously polarized (ap) bands. Only one depolarized (dp) band is tentatively identified (1619 cm^{-1}). The absence of dp bands in the RR spectrum suggests that the actual symmetry of CuOEiBC is less than C_2; however, the symmetry is not sufficiently low that all bands become polarized. The depolarization ratios, ρ, for the p bands are in the range of $\sim$ 0.2–0.6 although the ρ's for most of these bands are 0.4–0.5. The ρ's for the ap modes are typically in the range of 1.0–3.0. The exact ρ values depend on the excitation wavelength as expected for a molecule of low symmetry that exhibits a number of absorption bands in close proximity.[30] In general, the polarization patterns indicate that both Franck–Condon and Herzberg–Teller scattering mechanisms are active in the various resonant electronic excited states. This is reasonable considering that the B_x, B_y, and Q_y absorptions are comparable in intensity and relatively close in energy. Only Herzberg–Teller scattering should be observed from the weak Q_x transition. However, as was previously noted, the scattering from this state is most likely masked by scattering from the much stronger nearby absorptions, notably Q_y.

B. IR Spectra. The solution IR spectra of CuOEiBC and the three isotopomers are shown in Figure 6. Nearly all of the skeletal fundamentals observed in the IR spectra of the complexes have counterparts in the RR spectra. This is expected in a complex of relatively low symmetry where all modes are formally RR and IR allowed.[30] However, there are several important exceptions to the mutual RR and IR activity exhibited by the skeletal modes of CuOEiBC. In particular, the isotopic shift patterns indicate that the 1616- and 1562-cm^{-1} IR bands are not due to the same modes as those that give rise to the 1621- and 1557-cm^{-1} RR bands. *meso*-Deuteriation does not shift the 1616 (IR)- and 1557 (RR)-cm^{-1} bands whereas it does shift the 1621 (RR)- and 1562 (IR)-cm^{-1} bands (Figures 3, 4, and 6). Finally, it should be noted that a number of the skeletal-mode IR bands exhibit substantially different frequencies (by as much as 6 cm^{-1}) in solution versus solid phase. This again emphasizes the necessity of comparing vibrational data acquired under similar conditions.

C. Vibrational Assignment and Normal Mode Descriptions. The observed and calculated frequencies and normal mode descriptions for the high-frequency, in-plane skeletal modes of CuOEiBC are listed in Table I along with the observed and calculated *meso*-deuteriation shifts. The polarizations of the RR bands are also given in the table. All observed and calculated fundamental modes

Table I. Observed and Calculated Frequencies (cm^{-1}) of the In-Plane Skeletal Modes for CuOEiBC

	obsd[a]				$\Delta\gamma$-d_1		$\Delta\beta,\gamma,\delta$-$d_3$		$\Delta\alpha,\beta,\gamma,\delta$-$d_4$		
no.	RR	IR	calcd	sym	obsd	calcd	obsd	calcd	obsd	calcd	assignment[b]
1	1651 (ap)	1651	1656	B	1	2	8	7	8	13	$\nu C_aC_m(\beta,\delta)$
2	1621 (p)		1640	A	1	0	14	15	14	15	$\nu C_aC_m(\beta,\delta)$
3	1619 (dp)[c]		1593	B	14	14	26	21	26	24	$\nu C_aC_m(\gamma,\beta,\delta)$
4		1616	1598	A	0	0	3	3	3	6	νC_bC_b(I,II)
5		1562	1637	B	1	4	9	9	9	15	$\nu C_aC_m(\beta,\delta)$
6	1557 (p)		1559	B	1	0	1	5	1	6	νC_bC_b(I,II)
7	1527 (ap)	1527	1460	B	0	1	19	8	23	15	$\nu C_aC_m(\alpha,\beta,\delta)$, νC_bC_b(I,II)
8	1512	1512	1528	A	0	0	8	4	8	5	$\nu C_aC_m(\beta,\delta)$
9	1496 (p)	1496	1487	B	1	0	2	2	2	3	νC_aC_b(I,II)
10	1481 (p)	1481	1510	A	2	0	7	3	7	8	$\nu C_aC_m(\beta,\delta)$
11			1479	A		13		15		15	$\nu C_aC_m(\gamma)$
12	1402 (p)		1452	A	0	0	0	3	0	2	νC_aC_b(I,II), νC_aN(I,II)
13	1390 (p)		1406	A	0	0	17	10	17	14	νC_aN(I,II,III,IV), νC_aC_b(I,II)
14		1409	1359	A	0	0	8	15	8	16	νC_aN(I,II,III,IV)
15			1393	B		1		16		33	νC_aN(I,II,III,IV), νC_aC_b(I,II)
16			1362	B		100		66		63	$\delta C_mH(\gamma,\beta,\delta)$, νC_aN(I,II,III,IV)
17	1320 (ap)	1320	1354	B	0	+3		445		451	$\delta C_mH(\beta,\delta)$
18	1306 (p)		1329	A	0	0		391		392	$\delta C_mH(\beta,\delta)$
19			1319	B		+6		+6		192	$\delta C_mH(\alpha)$, νC_aC_b(I,II)
20			1281	B		+13		+10		+10	δC_bH(III,IV)
21			1280	A		0		+4		+4	δC_bH(III,IV)
22			1278	B		0		1		4	δC_bH(III,IV)
23			1277	A		0		3		0	δC_bH(III,IV)
24	1226		1222	A	0	0	+12	+14	+12	+14	νC_aC_b(III,IV)
25			1237	B		96		158		195	$\delta C_mH(\gamma,\beta,\delta)$
26	1207		1213	B	0	+5		+21		+24	γC_bH(III,IV), νC_aC_b(III,IV)
27			1174	A		0		1		1	δC_bH(III,IV), νC_aC_b(III,IV)
28		1184	1089	B	2	50	+92	+97	+92	+105	νC_aN(III,IV), νC_aC_b(III,IV)
29	1174 (ap)		1156	B	1	+8	+17	+7	+17	+7	νC_aC_b(III,IV), νC_aN(III,IV)
30	1150 (p)		1129	A	1	0	+18	+27	+18	+26	νC_aC_b(III,IV), δC_bH(III,IV)

[a] Abbreviations: p, polarized; ap, anomalously polarized; dp, depolarized; sh, shoulder. [b] Mode descriptions are as follows: ν = stretch, δ = in-plane deformation, and γ = out-of-plane deformation. C_a, C_b, C_m and the characters refer to the macrocyclic positions shown in Figure 1. [c] Observed in polarized Q-state-excitation RR spectra.

with frequencies above 1000 cm^{-1} are listed. The isotopic shift data allow the assignments for the modes above 1250 cm^{-1} to be made with a reasonable degree of certainty. The assignments in the range 1000–1250 cm^{-1} are less certain due to the increased spectral congestion and complicated isotopic-shift patterns (vide infra). Modes below 1000 cm^{-1} are not listed in Table I because the correlations between the observed spectra and vibrational frequencies calculated via the QCFF/PI method are ambiguous.

IV. Discussion

A. Vibrational Assignments. The vibrational assignments listed in Table I were determined by using the observed *meso*-deuteriation shifts and RR polarizations in conjunction with the frequencies, deuteriation shifts, and mode symmetries predicted by the semiempirical normal coordinate calculations. The assignment process for CuOEiBC was also guided by the general frequency characteristics exhibited by C_aC_m, C_bC_b, C_aC_b, and C_aN stretching and C_mH in-plane bending modes of metalloporphyrins[57-60] and metallochlorins.[30-41] The semiempirical nature of the normal coordinate calculations dictates that the absolute frequencies of certain modes differ substantially from those observed. Consequently, calculated isotopic shifts were given more weight in determining the assignments than were the frequencies. The specific assignments for these modes are discussed in more detail below.

1. C_aC_m and C_bC_b Modes. The eight C_aC_m stretching vibrations of CuOEiBC are RR and IR allowed (4 A and 4 B) due to the low symmetry of the complex. On the basis of the spectral analysis and normal coordinate calculations, the six RR bands of CuOEiBC observed at 1651 (ap), 1621 (p), 1619 (dp), 1527 (ap), 1512, and 1481 (p) cm^{-1} are attributed to these stretching motions. The modes at 1651, 1527, 1512, and 1481 cm^{-1} also exhibit IR activity whereas those at 1621 and 1619 cm^{-1} do not. However, another C_aC_m vibration, which only exhibits IR activity, is observed at 1562 cm^{-1}. The remaining C_aC_m mode is predicted to occur at 1479 cm^{-1}. A moderately intense band is observed in both the RR and IR spectra at 1496 cm^{-1} that could be this C_aC_m mode. However, this band exhibits essentially no *meso*-deuteriation shift (2 cm^{-1} or less). Consequently we have assigned the 1496-cm^{-1} band to a C_aC_b mode that is also predicted to lie in this region. This latter assignment is somewhat problematic in that the calculated C_aC_b vibration is nontotally symmetric whereas the RR band is polarized ($\rho \sim 0.3$). However, this can be rationalized if the actual symmetry of the macrocycle is lower than C_2 (vide supra).

The four C_bC_b stretching modes (2 A and 2 B) are both Raman and IR allowed. Two high-frequency modes are observed that exhibit *meso*-deuteriation shifts commensurate with those expected for C_bC_b vibrations, an IR band at 1616 cm^{-1}, and a RR band at 1557 (p) cm^{-1}. We have assigned these two bands as the A- and B-type C_bC_b modes, respectively, despite the fact that the lower frequency band is polarized ($\rho \sim 0.3$–0.5, depending on the excitation wavelength). A reversed assignment, which is nominally more consistent with the IR and RR activity of the two modes and with the RR polarization data (presuming C_2 symmetry), is at odds with the calculated frequency ordering for the two C_bC_b vibrations and, more importantly, with the frequency ordering observed and calculated for the C_bC_b stretches of all MOEP and MOEC complexes.[30,37,41,57-60] For these latter macrocycles, a totally symmetric C_bC_b vibration is the highest in energy. The absence of RR activity for the in-phase C_bC_b stretch of CuOEiBC is not expected; however, the totally symmetric C_bC_b stretch of CuOEC is not observed in the RR spectrum[42] (Babcock and co-workers have recently shown that a RR

(57) Abe, M.; Kitagawa, T.; Kyogoku, Y. *J. Chem. Phys.* **1978**, *69*, 4526–4534.
(58) Li, X.-Y.; Czernuszewicz, R. S.; Kincaid, J. R.; Stein, P.; Spiro, T. G. *J. Phys. Chem.* **1990**, *94*, 47–61.
(59) Kitagawa, T.; Ozaki, Y. *Structure Bonding* **1987**, *64*, 71–114.
(60) (a) Spiro, T. G. In *Iron Porphyrins*; Lever, A. P. B., Gray, H. B., Eds.; Addison-Wesly: Reading, MA, 1983; Part II, pp 89–159. (b) Spiro, T. G.; Czernuszewicz, R. S.; Li, X.-Y. *Coord. Chem. Rev.* **1990**, *100*, 541–571. (c) Felton, R. H.; Yu, N.-T. In *The Porphyrins*; Dolphin, D., Ed.; Academic Press: New York, 1978; Vol. 3, pp 347–393.

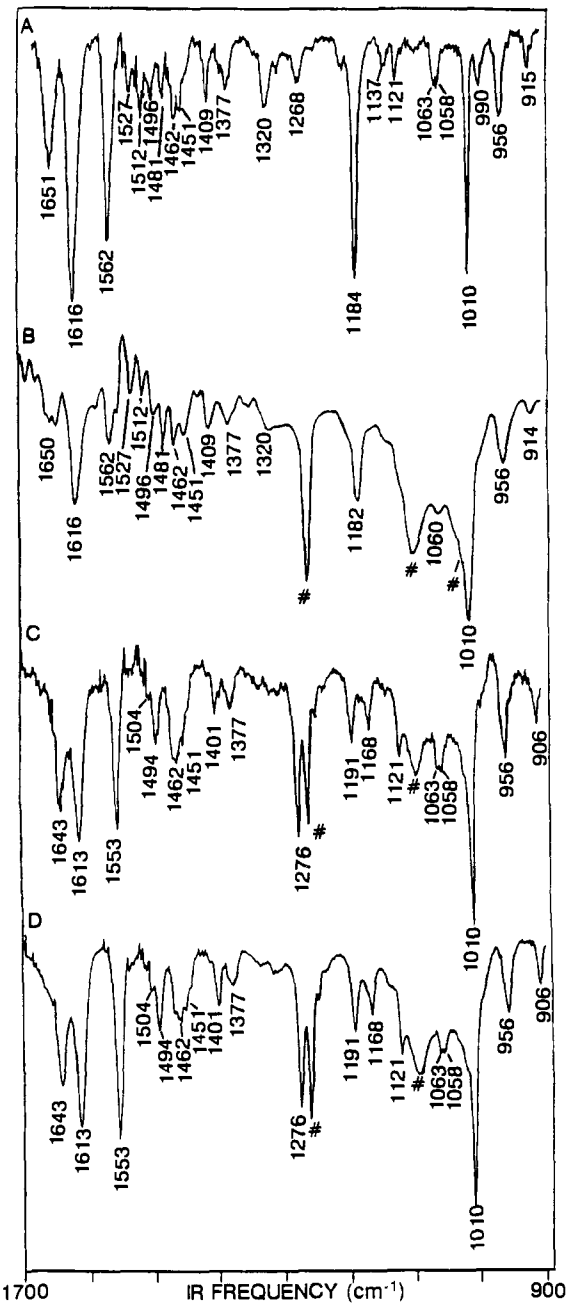

Figure 6. IR spectra of (A) CuOEiBC, (B) CuOEiBC-γ-d_1, (C) CuOEiBC-β,γ,δ-d_3, and (d) CuOEiBC-$\alpha,\beta,\gamma,\delta$-$d_4$. The spectra are of samples in CCl_4 solution. The peaks labeled by the symbol # in the spectra of the deuteriated complexes are due to trace impurities of silicone grease.

band previously assigned as the totally symmetric C_bC_b vibration[31] of CuOEC is actually a C_aC_m vibration). The other two C_bC_b vibrations of CuOEiBC involving the reduced rings are calculated at 981 (A) and 964 (B) cm^{-1}, respectively. No bands are observed in either the RR or IR spectra that can be assigned to these vibrations.

The computed vibrational eigenvectors for the C_aC_m motions of CuOEiBC are plotted in Figure 7 (rows a and b). Displacements are shown only for those atoms whose motions contribute significantly to the normal mode (10% or greater of the maximum displacement of a given mode). The calculations predict that certain of the C_aC_m vibrations are relatively localized on particular methine bridges while others are more delocalized. The pattern of the observed *meso*-deuteriation shifts confirms this general prediction; however, the calculated and observed shift patterns are in much better accord for certain modes than for others. For example, the calculations indicate that modes 2 and 8 are localized in the β,δ-methine bridges while modes 3 and 7 contain γ- or α-methine character, respectively, in addition to β,δ-methine character. These predictions are in general accord with the observed *meso*-deuteriation-shift patterns. On the other hand, modes 1 and 5 are predicted to contain more α-methine character than appears consistent with the observed *meso*-deuteriation shifts.

The vibrational eigenvectors for the four C_bC_b stretches are shown in Figure 7 (row c). The calculations predict that both of the high-frequency C_bC_b stretches contain a reasonable amount of C_aC_m character. However, the *meso*-deuteriation shifts observed for the two bands indicate that the actual contribution of C_aC_m motion is less than that predicted. This is particularly the case for mode 6 whose shifts are commensurate with essentially pure C_bC_b character.

2. C_aC_b and C_aN Modes. The eight C_aC_b and C_aN modes of CuOEiBC are RR and IR allowed (4 A and 4 B for each mode type). The normal coordinate calculations indicate that these two types of vibrations are extensively mixed with one another and with other motions of the macrocycle. This is also the case in metalloporphyrins and metallochlorins.[39,37,41,57-60] The vibrational modes which contain substantial C_aC_b and C_aN motions occur predominantly in the 1000–1400-cm^{-1} spectral region. Three prominent RR bands that can be attributed to C_aC_b and/or C_aN vibrations are observed at 1496 (p), 1402 (p), and 1390 (p) cm^{-1}. The 1496-cm^{-1} band is also observed in the IR as is another C_aN mode at 1409 cm^{-1}. The calculated vibrational eigenvectors for these four (and four other) C_aC_b/C_aN modes are shown in Figure 8 (rows a and b). Comparison of the vibrational eigenvectors of the C_aC_b and C_aN modes of CuOEiBC with those of MOEP[57,58] reveals that none of the vibrational modes can be explicitly correlated for the two types of macrocycles. However, mode 13 of CuOEiBC most nearly resembles the ν_4 oxidation-state marker band of iron porphyrins. In this regard, Spiro and co-workers have observed a strong RR band near 1384 cm^{-1} in the spectra of $(OEiBCFe)_2O$ which they have attributed to the analogue of ν_4.[51]

3. In-Plane C_mH Modes. All four in-plane C_mH deformations are RR and IR allowed for CuOEiBC (1 A and 3 B). However, the RR spectra exhibit only two bands, 1320 (ap) and 1306 (p) cm^{-1}, of moderate to low intensity that can be identified as in-plane C_mH deformations. Only the 1320-cm^{-1} vibration exhibits substantial IR activity. In the case of the *meso*-deuteriated complexes, no RR or IR bands can be identified as C_mD deformations. These modes are typically expected in the region below 1000 cm^{-1} and are fairly weak.[57,58] The relatively low RR activity observed for the C_mH deformations of CuOEiBC can be contrasted with the much stronger activity observed for these modes in MOEP and MOEC complexes.[31,32,37,38,42,57-60]

The vibrational eigenvectors of four modes that are predicted to contain a significant amount of C_mH motion are shown in Figure 8 (row c). As is the case for the C_aC_m stretching vibrations, the C_mH deformations are to a certain degree localized on specific methine bridges. For CuOEiBC, the single totally symmetric deformation, mode 18, is restricted to the β,δ-methine bridges by symmetry. This constraint does not apply to the three nontotally symmetric C_mH vibrations; however, the RR band assigned as the only observed B-symmetry mode, No. 17, does not shift upon γ-deuteriation. Accordingly, this deformation is at least partially localized on the β,δ- or α,β,δ-methine bridges.

The normal coordinate calculations indicate that the C_mH deformations are substantially mixed into a large number of modes in the 1000–1400-cm^{-1} spectral region. This leads to an extraordinarily complicated pattern of deuteriation shifts. With each successive addition of a deuteron, a number of modes (typically 3–5) exhibit significant changes in the general form of their eigenvectors. These changes are accompanied in several cases by significant upshifts, particularly of bands in the 1100–1200-cm^{-1} regime (Nos. 28–30). This type of upshifting upon *meso*-deuteriation is also observed in porphyrins and chlorins and is typically attributed to an uncoupling of the C_mH deformations from certain motions of the ring skeleton.[37,41,42,57,58] However, when the forms of the eigenvectors of a number of skeletal modes change upon deuteriation, it is generally not appropriate to make one-to-one

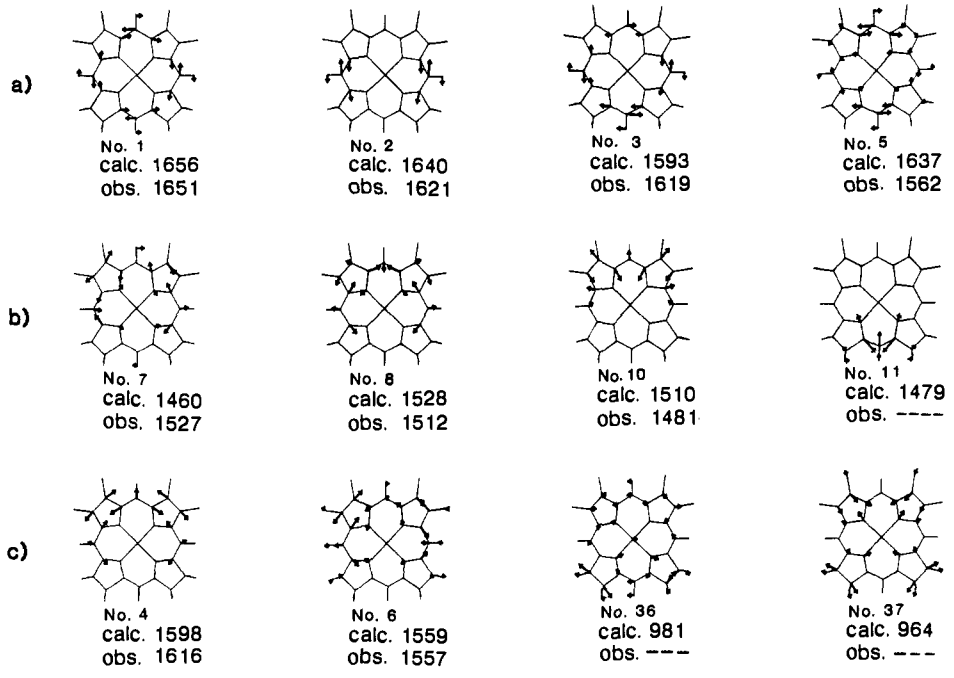

Figure 7. Vibrational eigenvectors of CuOEiBC which contain substantial contributions from C_aC_m (rows a and b) and C_bC_b (row c) stretching motions. The pyrroline rings are at the bottom of the macrocycle.

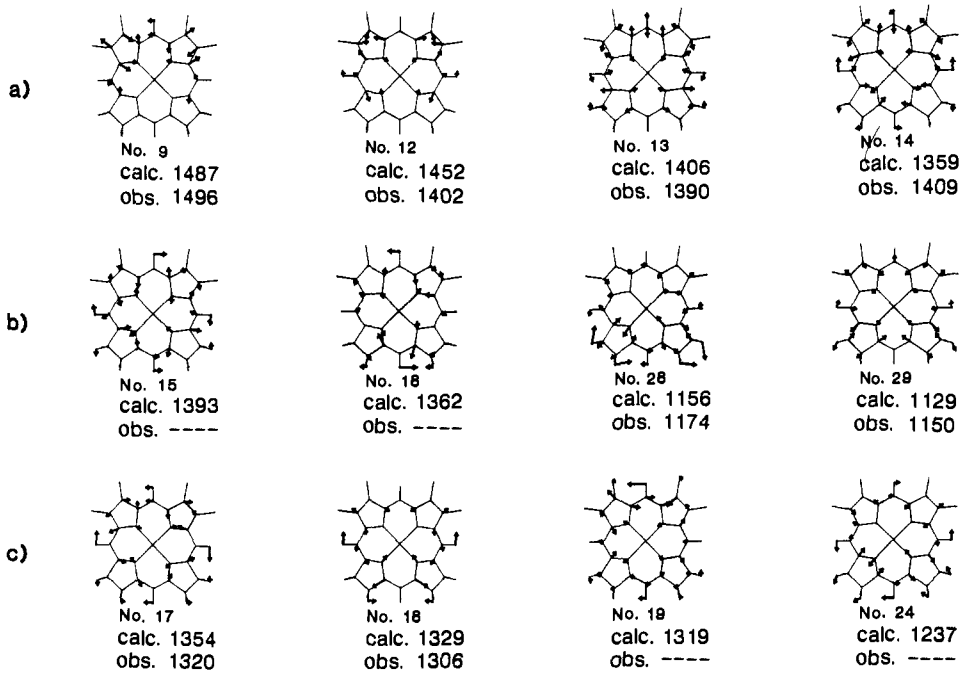

Figure 8. Vibrational eigenvectors of CuOEiBC which contain substantial contributions from C_aN and C_aC_b (rows a and b) stretching motions and C_mH deformations (row c). The pyrroline rings are at the bottom of the macrocycle.

correlations between the vibrations of *meso*-protonated and *meso*-deuteriated macrocycles.[37] Instead, such changes indicate that the most accurate representation of the effects of deuteriation is that several modes are transformed into several others. The eigenvectors calculated for CuOEiBC and the three different isotopomers indicate that this is clearly the case for this macrocycle. Consequently, the one-to-one mode correlations listed in Table I should be considered approximate.

4. Other Modes. Certain modes that contain contributions from C_b-ethyl stretching motions and internal vibrations of the ethyl groups are expected in the spectral region above 1000 cm^{-1}.[57-61] These modes make a substantial contribution to the IR spectra of tetrapyrrolic macrocycles.[61] In the case of CuOEiBC, we attribute the IR bands observed at 1462, 1451, 1377, 1121, 1063, 1058, and 1010 cm^{-1} to internal vibrations of the ethyl groups. The assignments of these modes are based on their insensitivity to *meso*-deuteriation and on correlations with the observed and calculated frequencies of these modes of MOEP complexes.[58,61]

Until recently, internal vibrations of the ethyl groups were not thought to contribute to the RR spectra of ethyl-substituted tetrapyrrolic macrocycles. However, Spiro and co-workers have shown through extensive deuteriation studies that such modes are in fact observed in the RR spectra of MOEP complexes.[58] We have tentatively assigned the CuOEiBC RR bands observed at 1462, 1269, 1026, and 1010 cm^{-1} as ethyl group vibrations based on their insensitivity to *meso*-deuteriation and the close correspondence in their frequencies with ethyl-mode RR bands of

(61) Kincaid, J. R.; Urban, M. W.; Watanabe, T.; Nakamoto, K. *J. Phys. Chem.* **1983**, *87*, 3096-3101.

MOEP complexes.[58] Certain of the ethyl-group RR bands of CuOEiBC are quite intense (for example the 1010- and 1026-cm^{-1} bands) as is also the case for MOEP modes in this spectral region.[58-60] This observation indicates that these motions are substantially mixed with the skeletal modes of the OEiBC macrocycle. It is not obvious whether this mixing occurs in both the ground and resonant excited electronic states or is confined primarily to only one of the two.

B. Effects of Low Symmetry on the Electronic and Vibrational Structure. The reduction of two of the pyrrole rings of a metalloporphyrin significantly affects the electronic properties of the molecule. The degenerate B and Q states of the macrocycle are split and the lowest energy state, Q_y, gains appreciable oscillator strength (Figure 2). The significant oscillator strength in Q_y, B_x, and B_y results in the observation of both Franck–Condon and Herzberg–Teller scattering in the RR spectra of CuOEiBC with excitation at all wavelengths in the B and Q absorption regions. Detailed RR excitation profiles are not available for any isobacteriochlorins; consequently, the exact nature of the excited-state couplings is uncertain. However the complexity of the couplings is evidenced by the fact that the ρ values for all bands vary appreciably with excitation wavelength. The close proximity of the B_x and B_y states suggests that vibronic coupling between these states should be particularly strong. However, comparison of Figures 3 and 4 reveals that the number and intensities of nontotally symmetric modes are approximately equal with B- and Q-state excitation. This observation suggests that B–Q vibronic coupling may in fact be much stronger than B_x–B_y coupling.

In the case of an isobacteriochlorin, the reduction of adjacent pyrrole rings dictates that the transition dipoles are rotated by ~45° with respect to those of chlorins or bacteriochlorins. The general effects of this axis rotation have been previously discussed.[30,51] The salient consequence is that the B_{1g} and B_{2g} modes of metalloporphyrins, which become A and B modes in metallochlorins, are instead B and A modes in metalloisobacteriochlorins. For metalloporphyrins, the RR enhancements of the B_{1g} modes are generally much larger than those of the B_{2g} vibrations.[57-60] The observation that there are a relatively large number of nontotally symmetric (namely ap) versus totally symmetric modes in the RR spectra of CuOEiBC suggests that these additional B symmetry modes are derived (at least qualitatively) from B_{1g} porphyrinic vibrations. It should be emphasized that all of the above symmetry arguments are approximate because the polarization patterns (absence of dp modes) suggest that CuOEiBC has less than C_2 symmetry.

The low symmetry of CuOEiBC in conjunction with the potentially complicated nature of the excited-state vibronic coupling may also be responsible for the unusual intensity enhancement patterns observed for certain modes upon *meso*-deuteriation. This is strikingly illustrated by the enhancement pattern exhibited by the 1390-cm^{-1} band. With B-state excitation (Figure 3), the intensity of this RR band is approximately the same for all four isotopomers. In contrast, the Q-state excitation (Figure 4), the intensity of this band in CuOEiBC-β,γ,δ-d_3 and CuOEiBC-$\alpha,\beta,\gamma,\delta$-$d_4$ is drastically reduced compared with that observed for the normal isotopomer or CuOEiBC-γ-d_1. In the case of CuOEiBC-β,γ,δ-d_3 and CuOEiBC-$\alpha,\beta,\gamma,\delta$-$d_4$, deuteriation downshifts the 1390-cm^{-1} band (No. 13) away from the strong, nearby 1402-cm^{-1} band (No. 14) whereas the 1390-cm^{-1} band is not shifted in CuOEiBC-γ-d_1. The diminution in RR intensity observed for mode 13 upon tri- and tetra-*meso*-deuteriation does not appear to be due to a simple redistribution of intensity with the 1402-cm^{-1} band. The intensity of this latter band is approximately constant (relative to other bands in the spectrum) in all four isotopomers.

The low symmetry of CuOEiBC is the principal factor that alters the forms of the vibrational eigenvectors of this macrocycle relative to those of the more symmetrical MOEP complexes. The eigenvectors of the C_bC_b and C_aC_b vibrations are strongly perturbed by the reduction of two pyrrole rings because the C_bC_b and C_aC_b bonds on the pyrroline rings of CuOEiBC are single bonds rather than partial double bonds as they are in MOEP complexes. The differences in the intrinsic force constants associated with pyrrolic versus pyrrolinic C_bC_b and C_aC_b stretching modes dictates that these internal coordinates on the two types of rings make widely disparate contributions to any particular normal mode. This is clearly seen in the vibrational frequencies and eigenvectors of the C_bC_b vibrations of CuOEiBC. These modes are localized in pairs on either the pyrrolic or pyrrolinic rings and separated in frequency by hundreds of wavenumbers.

Although the C_aC_m and C_aN bonds of CuOEiBC possess partial double-bond character, the eigenvectors of the C_aC_m and C_aN stretches of this complex are different from those of MOEP complexes. This is particularly evident for the C_aC_m vibrations. Both the normal coordinate calculations and the observed *meso*-deuteriation shift patterns for the various bridge-specifically deuteriated isotopomers indicate that certain of these modes are fairly localized in specific methine bridges whereas others are more delocalized. However, even the more delocalized C_aC_m vibrations do not contain equal contributions from the three symmetry inequivalent methine bridges. The differences in the forms of the C_aC_m eigenvectors of CuOEiBC relative those of MOEP complexes are undoubtedly due to the fact that the bond lengths in the methine bridges are significantly affected by reduction of the two pyrrole rings. X-ray crystallographic studies indicate that the lengths of the two symmetry equivalent C_aC_m bonds in the bridge between rings I and II are approximately 1.37 Å.[56,62-64] The lengths of the symmetry equivalent pair that bridge rings III and IV are also 1.37 Å. However, the C_aC_m bonds that connect the pyrrolic and pyrrolinic rings are inequivalent and quite disparate in length. The lengths of the C_aC_m bonds to the former rings are long (1.42 Å) while those to the latter are short (1.35 Å). This large disparity implies that the intrinsic force constants for the stretches of these two bonds are quite different. This in turn should perturb the vibrational coupling between these methine bridges (β,δ) and the other two symmetry inequivalent methine bridges (α and γ).

The reduction of the two pyrrole rings also introduces bond length disparities in the C_aN bonds of tetrahydroporphyrin macrocycles.[56-62-64] The influence of these bond-length alterations on the vibrational eigenvectors of the C_aN vibrations is less easily visualized than is that on the C_aC_m vibrations because the former modes are appreciably mixed with other types of motions. Regardless, the effects of symmetry reduction are apparent in the behavior of certain C_aN vibrations of tetrahydroporphyrins versus porphyrins. For example, the siroheme mode nominally correlated with the ν_4 oxidation-state marker band of Fe porphyrins (mode 13 for CuOEiBC, Table I) does not, in fact, appear to be a good marker for the oxidation state of the Fe ion in tetrahydroporphyrins.[50,51]

V. Conclusions

The specific deuteriation studies and the normal coordinate calculations reported herein indicate that the forms of the vibrational eigenvectors of the OEiBC macrocycle are different from those of porphyrins (and also from those of chlorins or bacteriochlorins). These differences are a natural consequence of symmetry reduction and can be related to changes in the geometrical structure that occur upon hydrogenation of two of the pyrrole rings. The exact characteristics of the eigenvectors of isobacteriochlorins and hydroporphyrins in general can only be fully elucidated by studies of a variety of isotopomers that are designed to probe in a systematic fashion each structurally inequivalent portion of the macrocycle. The investigation of a number of isotopomers is particularly important for macrocycles such as isobacteriochlorins because these molecules possess low symmetry and there are large differences in the structures of the inequivalent portions of the ring. Collectively these results indicate that previous assignments of the vibrational spectra of siroheme

(62) Barkiga, K. M.; Fajar, J.; Chang, C. K.; Williams, G. J. B. *J. Am. Chem. Soc.* **1982**, *104*, 315–317.
(63) Barkiga, K. M.; Fajar, J.; Spaulding, C. D.; Williams, G. J. B. *J. Am. Chem. Soc.* **1981**, *103*, 176–181.
(64) Kratky, C.; Angst, C.; Eigill, J. *Angew. Chem., Int. Ed. Engl.* **1981**, *20*, 211–212.

and other metalloisobacteriochlorins should be reassessed.

Finally, it should be noted that the difference in the forms of the vibrational eigenvectors of OEiBC versus OEP (or versus other types of macrocycles) does not imply that the skeletal-mode frequencies of hydroporphyrins are any less sensitive to the structure of the ring than those of porphyrins. Instead, the differences in the eigenvectors suggest that the frequency–structure correlations are different between the ring systems. This is inherently reasonable in view of the substantial structural differences between these various classes of macrocycles.

Acknowledgment. This work was supported by Grant GM-36243 (D.F.B.) from the National Institute of General Medical Sciences.

Photolysis of Covalent Compounds Composed of Stable Anions and Cations. Transient Absorption Studies on Coordination Complexes Formed from the Triphenylcyclopropenyl Cation and Malonitrilo, Acetonitrilo, and Fluorenyl Anions

Norbert J. Pienta,*,† Robert J. Kessler,† Kevin S. Peters,‡ Erin D. O'Driscoll,‡ Edward M. Arnett,§ and Kent E. Molter§

Contribution from the Department of Chemistry, University of North Carolina, Chapel Hill, North Carolina 27599-3290, Department of Chemistry and Biochemistry, University of Colorado, Boulder, Colorado 80309-0215, and Department of Chemistry, Duke University, Durham, North Carolina 27706. *Received February 8, 1990. Revised Manuscript Received January 14, 1991*

Abstract: A series of molecules (1,2,3-triphenylcyclopropene (**1**), [3-(1,2,3-triphenylcyclopropenyl)](4′-cyanophenyl)malonitrile (**2**), [3-(1,2,3-triphenylcyclopropenyl)](4′-nitrophenyl)malonitrile (**3**), [3-(1,2,3-triphenylcyclopropenyl)](3′-nitrophenyl)malonitrile (**4**), [3-(1,2,3-triphenylcyclopropenyl)](4′-nitrophenyl)acetonitrile (**5**), and [3-(1,2,3-triphenylcyclopropenyl)]-9′-cyanofluorene (**6**), each composed of a stable carbanion and carbocation covalently attached to each other, has been photolysed with use of picosecond and nanosecond laser techniques. These molecules undergo a sequence of events that begins with absorption of a photon by one of two localized chromophores in each precursor (i.e., the stilbene of TPCP or the aryl portion of the starting carbanion). The singlet excited states initiate an electron transfer event at rates that were too fast to measure under the conditions employed. (The radical ions were observed within the shortest available time scale, ca. 25 ps.) The radical ion pairs have two possible alternatives: (1) back electron transfer to form the triplet excited state of the triphenylcyclopropenyl part and (2) bond fragmentation of the central bond (i.e., the one connecting the carbanion to the carbocation). Apparently, the presence of ions from the latter fragmentation depends on the relative rates of the two processes.

Radical and ion intermediates play a critical role in mechanistic organic chemistry. In the last few years, one of us has established a research effort that is investigating aspects that control the equilibria among the three states: the pair of cations C^+ and A^-, the pair of radicals $C^\bullet$ and $A^\bullet$, and the covalent complex C–A (Scheme I).[1] As a result, both thermodynamic and kinetic data are available for a variety of complexes that undergo spontaneous heterolysis and homolysis in solution at room temperature. The previous studies have described the behavior of a wide variety of systems at or near their equilibria. Data include the equilibrium constants, enthalpies to form the central bond, and rates of bond fragmentation and coordination. In the present study, a number of these compounds and related ones have been photolyzed in an attempt to access the radicals and ions at a point far from equilibrium with their covalent precursors. Thus, in this paper, data are included for a series of related complexes (C–A, where C and A refer to the cation and anion from which the starting materials are made):[2] 1,2,3-triphenylcyclopropene (**1**), [3-(1,2,3-triphenylcyclopropenyl)](4′-cyanophenyl)malonitrile (**2**), [3-(1,2,3-triphenylcyclopropenyl)](4′-nitrophenyl)malonitrile (**3**), [3-(1,2,3-triphenylcyclopropenyl)](3′-nitrophenyl)malonitrile (**4**), [3-(1,2,3-triphenylcyclopropenyl)](4′-nitrophenyl)acetonitrile (**5**), [3-(1,2,3-triphenylcyclopropenyl)]-9′-cyanofluorene (**6**) (Figure 1).

The use of picosecond laser techniques enables comprehensive studies on the crossing of excited-state potential surfaces with those for homolytic and heterolytic bond cleavage.[3] Analogous nanosecond techniques bridge the time frame between the picosecond experiments (in which we can and do observe excited states and

Scheme I. Equilibria among Coordination Complex, Ion Pair, and Radical Pair

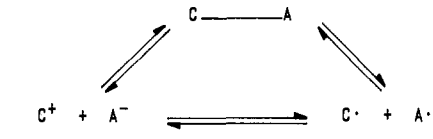

† University of North Carolina.
‡ University of Colorado.
§ Duke University.

(1) (a) Arnett, E. M.; Troughton, E. B. *Tetrahedron Lett.* **1983**, *24*, 3229. (b) Arnett, E. M.; Troughton, E. B.; McPhail, A.; Molter, K. E. *J. Am. Chem. Soc.* **1983**, *105*, 6172. (c) Troughton, E. B.; Molter, K. E.; Arnett, E. M. *Ibid.* **1984**, *106*, 6726. (d) Arnett, E. M.; Chawla, B.; Molter, K. E.; Amarnath, K.; Healy, M. *Ibid.* **1985**, *107*, 5288. (e) Arnett, E. M.; Molter, K. E. *J. Phys. Chem.* **1986**, *90*, 471. (f) Arnett, E. M.; Molter, K. E. *Acc. Chem. Res.* **1985**, *18*, 339. (g) Arnett, E. M.; Molter, K. E.; Marchot, E. C.; Donovan, W. H.; Smith, P. *J. Am. Chem. Soc.* **1987**, *109*, 3788. (h) Arnett, E. M.; Whitesell, L. G., Jr.; Cheng, J.-P.; Marchot, E. C. *Tetrahedron Lett.* **1988**, *29*, 1507. (i) Arnett, E. M.; Amarnath, K.; Harvey, N. G.; Cheng, J.-P. *J. Am. Chem. Soc.* **1990**, *112*, 344.

(2) For the compounds reported herein, C = 1,2,3-triphenylcyclopropenyl, or TPCP for short. The incipient anionic portions A are (4-cyanophenyl)-malonitrilo, CMN; (4-nitrophenyl)malonitrilo, NMN; (3-nitrophenyl)malonitrilo, MET; (4-nitrophenyl)acetonitrilo, NAN; 9-cyanofluorenyl, CFL; and hydrogen, H. Covalent compounds will appear as C–A (e.g., TPCP–CMN), while the intermediates will be drawn as C^+ or $A^\bullet$ (e.g., $TPCP^+$ or $CMN^\bullet$). The term "coordination complex" is the accepted nomenclature for the covalent molecules denoted as C–A (see ref 1).

(3) Peters, K. S. *Ann. Rev. Phys. Chem.* **1987**, *38*, 253–70 and references cited therein.

0002-7863/91/1513-3773$02.50/0